Linear Dichroism and the Transition Dipole Moment Orientation of the Carotenoid in the LH2 Antenna Complex in Membranes of Rhodopseudomonas acidophila Strain 10050

ARTICLE · DECEMBER 2001

DOI: 10.1021/jp010271b · Source: OAI

Linear Dichroism and the Transition Dipole Moment Orientation of the Carotenoid in the LH2 Antenna Complex in Membranes of *Rhodopseudomonas acidophila* Strain 10050

Pamela M. Dolan,[†] Deborah Miller,[†] Richard J. Cogdell,[‡] Robert R. Birge,[†] and Harry A. Frank*,[†]

Department of Chemistry, University of Connecticut, Storrs, Connecticut 06269-3060, and Division of Biochemistry and Molecular Biology, Institute of Biomedical and Life Sciences, University of Glasgow, Glasgow G128QQ, United Kingdom

Received: January 23, 2001; In Final Form: August 23, 2001

Linear dichroism (LD) of the carotenoid, rhodopin glucoside, and the 800 and 850 nm absorbing bacteriochlorophylls in the LH2 antenna complex from membranes of *Rhodopseudomonas acidophila* strain 10050 squeezed in polyacrylamide gels is reported. A model is presented for computing the ratio of the LD-to-isotropic absorption (LD/A) for the pigments based on the crystal structure of the LH2 complex solved by X-ray diffraction methods. Semiempirical molecular orbital (MO) calculations have refined the structure of the protein-bound rhodopin glucoside and show that the transition moment of the carotenoid is not collinear with the long axis of the molecule. Rather, it is 9.1° off axis from the extended π-electron conjugated chain. This rotation of the transition moment vector away from the structural long axis emerges as a result of the single/double bond alternation naturally present in all polyenes and carotenoids and is not due to environmental perturbations induced by binding of the molecule to the pigment−protein complex. Calculations of the intensity of polarized absorption for the rhodopin glucoside molecule predict a significant effect of the magnitude of the off-axis angle on the value of the observed LD/A. This paper employs semiempirical MO calculations and seeks to correlate the experimentally observed LD, which gives the orientation of the transition moment of the rhodopin glucoside in the membranes, with the X-ray diffraction results, which reveals the molecular structure of the carotenoid to atomic resolution.

Introduction

Linear dichroism (LD) is the differential absorption of plane-polarized light by an ordered sample.[1,2] If the structure and orientation of a molecule are known relative to an external frame of reference, then LD can be used to determine the geometric relationship between the transition moment of the absorbing species and its molecular structure. For example, LD carried out on molecules in single crystals whose structures have been solved to atomic resolution using X-ray diffraction provides a method for determining the orientation of the absorbing transition moment with respect to the molecular axis system. If the geometric relationship between the transition moment and the molecular structure can be established independently, e.g., by symmetry considerations, then LD can be used to determine the orientation of molecular species. This approach has been used extensively to determine the orientations of chromophores in biological samples.[1] However, ambiguities arise when the symmetry is not sufficient to assign the transition moment direction with respect to the molecular frame. The problem is compounded by molecular interactions or distortions that can cause further reductions in the symmetry of the molecule. In these instances, deducing the transition moment orientation relative to the molecular frame is not easily accomplished. A case in point is the use of polarized light spectroscopy including LD and photoselection[2] to deduce the orientations of carotenoid molecules in membrane-bound pigment−protein complexes prepared from photosynthetic organisms.[3−8] The implicit assumption in the vast body of literature on this subject has been that the direction of the strongly allowed transition moment lies along the long axis of the π-electron conjugated chain; this axis is defined as a vector drawn from the first carbon in the conjugated system to the last. Recent experimental and computational studies have shown that the transition moment of polyenes and carotenoids is not collinear with the long molecular axis.[9] In fact, there is no symmetry requirement that this be the case. The off-axis angle can take on any value and still be consistent with the symmetry of the point group.[9] This systematic deviation of transition moment direction from the molecular axis system has not been taken into account in the use of LD to determine the geometries of carotenoid molecules in biological systems. Also, interactions between the chromophore and its environment in the protein or membrane may substantially twist or otherwise further distort the molecule. These effects need to be considered if accurate assessments of the geometries of carotenoids in biological samples are to be derived from LD data.

Extrapolation of experimental and theoretical results on simple polyenes[10−13] has given many clues into the electronic structure and photochemical behavior of carotenoids. Polyenes can be considered good model systems for carotenoids. They have relatively high fluorescence yields and, in some cases, display well-resolved vibronic features in their absorption and fluorescence spectra, which has facilitated the assignments of the state energies.[14−18] The data have provided a rich testing ground for

* To whom correspondence should be addressed. E-mail: harry.frank@uconn.edu.
[†] University of Connecticut.
[‡] University of Glasgow.

10.1021/jp010271b CCC: $20.00
Published on Web 11/07/2001

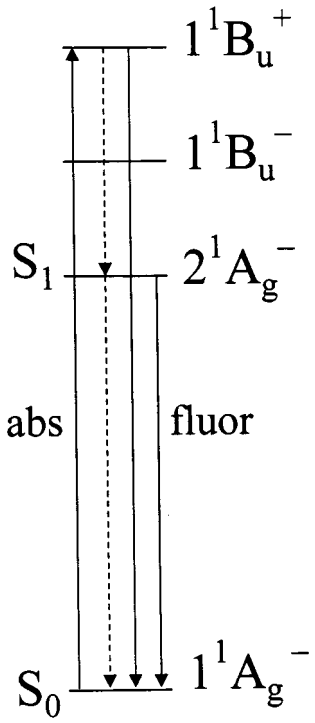

Figure 1. Energy level diagram showing the relative ordering of the excited singlet states and summarizing many of the photochemical properties of polyenes and carotenoids. The solid lines refer to the radiative transitions, absorption (abs), and fluorescence (fluor). The dashed lines refer to nonradiative internal conversion. Four singlet states are depicted as follows: the ground state, S_0, denoted $1^1A_g^-$; a low-lying excited singlet state denoted $2^1A_g^-$, referred to as S_1; a higher excited state labeled $1^1B_u^-$; and the $1^1B_u^+$ state into which absorption from the ground state is strongly allowed.

theoretical formalisms that seek to explain the spectroscopic properties and photochemical behavior of conjugated π-electron systems.

An energy level diagram that shows the relative ordering of the excited singlet states and also summarizes many of the photochemical properties of polyenes and carotenoids is given in Figure 1. In the figure, four singlet states are depicted as follows: (1) the ground state, S_0, also denoted $1^1A_g^-$ for its symmetry in the idealized C_{2h} point group; (2) a low-lying excited singlet state also of A_g symmetry, commonly referred to as S_1, and denoted $2^1A_g^-$; (3) a higher excited state labeled $1^1B_u^-$; and (4) the $1^1B_u^+$ state into which absorption from the ground state is strongly allowed. Many carotenoids do not have C_{2h} symmetry; yet, they tend to exhibit many of the spectroscopic and photochemical characteristics of the short, unsubstituted polyenes that do have C_{2h} symmetry. Thus, it is common to use the polyene labels for the electronic states of carotenoids.[19] The + and − signs accompanying the group theoretical designations are pseudoparity elements and are derived from π-electron molecular orbital (MO) pairing relationships when configuration interaction (CI) among singly excited configurations is included.[19−21] One-photon transitions between states having the either the same pseudoparity element or the same group theoretical parity are forbidden. The $1^1A_g^- \rightarrow 1^1B_u^+$ transition, however, is strongly allowed and is associated with the bright visible coloration of all carotenoid molecules.[22,23]

There are significant challenges in describing the excited state properties of long chain polyenes using theory. Providing adequate electron correlation and size consistency is computationally difficult for small polyenes and often intractable for large polyenes. The strongly allowed low-lying valence excited

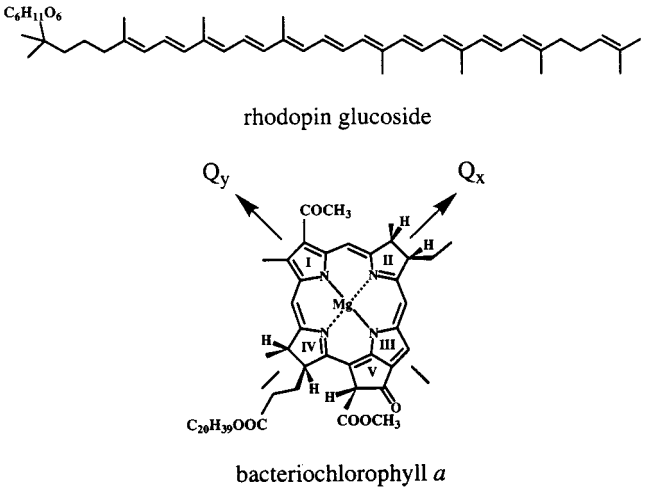

Figure 2. Structures of the rhodopin glucoside and BChl molecules. The directions of the Q_x and Q_y transition moments are indicated for BChl.

states can be described rather well using CI involving singly excited transitions.[20] The discovery of a lowest-lying forbidden state in the longer polyenes[24] demonstrated the need for higher levels of electron correlation, and in particular, the importance of doubly excited configurations in describing the covalent excited states.[25] Triple and quadruple CI are required to provide a size consistent basis set.[26,27] This observation is best demonstrated with respect to the present problem by reference to the energy separation between the lowest excited $2^1A_g^-$ state and the strongly allowed $1^1B_u^+$ state. This separation is observed experimentally to increase as the conjugation length of the polyene increases.[28] Theories that are limited to single and double CI, however, predict just the opposite. Indeed, a minimum of single, double, triple, and quadruple CI is required to provide an adequate level of size consistency and reproduce the experimental trends.[26,27] While such calculations are in principle possible for long chain polyenes, in practice, they are not because of both memory and processor limitations. We have addressed the problem of correlation and size consistency using a parametric approach to the electron mobility parameters, the repulsion integral, and the adjustment of the weights of the off-diagonal elements of the double-double CI matrix elements. These methods allow us to limit the CI basis set to singles and doubles, while providing a size consistent theory.[9,29−31]

In this paper, we report an investigation of the LD of the carotenoid, rhodopin glucoside, and bacteriochlorophyll (BChl) (Figure 2) bound in the LH2 complex in membranes from *Rhodopseudomonas acidophila* strain 10050. The structure of this pigment−protein complex has been solved to 2.5 Å resolution by X-ray diffraction.[32,33] (See Figure 3). The membranes have been oriented by squeezing in polyacrylamide gels.[8,34,35] The LD associated with the carotenoid and BChl absorption bands has been measured and is compared with that predicted from the crystal structure. Semiempirical MO calculations have been carried out using the coordinates of the rhodopin glucoside molecule obtained from the X-ray structure. The results reveal that the transition moment of the carotenoid lies 9.1° off the long structural axis of the molecule. This divergence from collinearity is shown to have a significant effect on the polarized light absorption spectra predicted from the coordinates of the crystal structure.

Materials and Methods

LH II Membrane Preparation. Cells of *R. acidophila* strain 10050 were grown photoheterotropically in Pfenning's medium

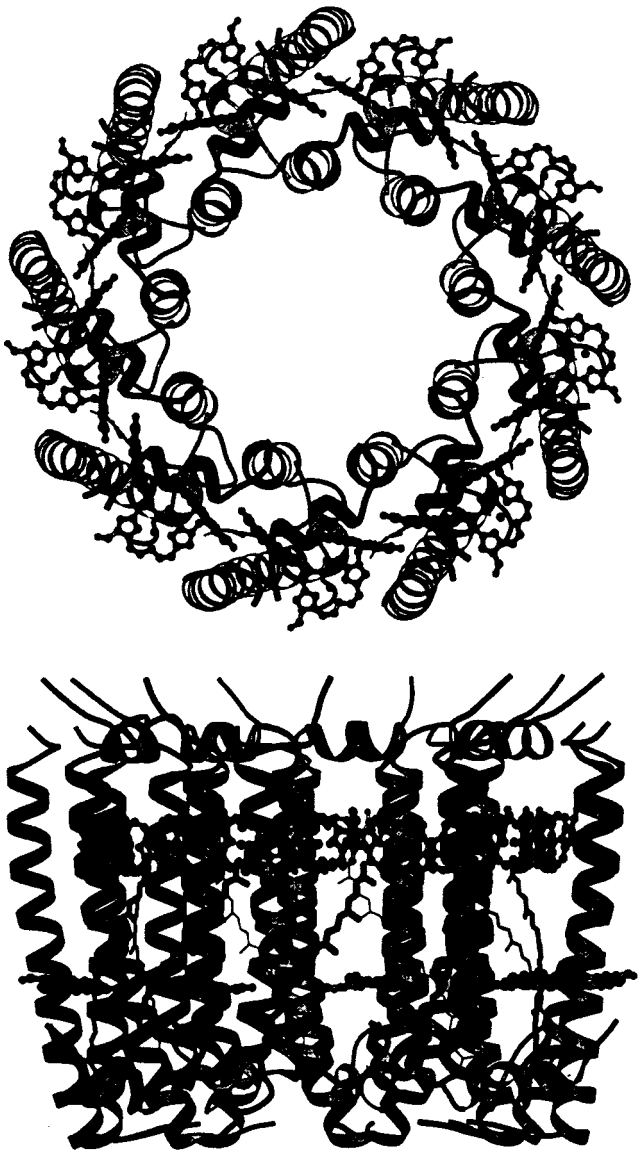

Figure 3. Structure of the LH2 complex from *R. acidophila* strain 10050. (Top) The circular nonameric complex viewed from one side of the membrane. The macrocycles of the 800 nm absorbing BChls lie in the plane of the membrane and are clearly visible in this view as are the cylindrical α-helical protein structures around the ring. (Bottom) Side view of the complex in the plane of the membrane. The 850 nm absorbing BChls are at the top of this figure. The long chain of the rhodopin glucoside follows a twisted sigmoidal path from these macrocycles to the bottom of the structure in this view.

from single colonies isolated on agar plates.[36] The batch cell cultures were grown under a 60 W incandescent bulb at 30 °C in 100 mL bottles and harvested by centrifugation at mid-log phase (OD 650 nm $\sim$ 0.5 cm^{-1}) after four transfers. The cells were resuspended in 100 mM KCl and 20 mM MES buffer at pH 6.8, disrupted by passage through a French press at 154 MPa in the presence of a small amount of DNAase and $MgCl_2$, and then resuspended in 20 mM Tris HCl buffer at pH 8. To minimize scattering, the broken membranes were solubilized using a 1:1 mixture of β-octylglucoside and lauryl-maltoside at a BChl:detergent ratio of 1:35 w/w. The membrane samples were then further purified using ultracentrifugation on a sucrose density gradient. Membranes prepared from cells grown under these conditions contain rhodopin glucoside as the sole carotenoid (Cogdell and Takaichi, unpublished data).

Gel Preparation. For the experiments carried out at room temperature, the gels contained the following final concentrations of components: 10% acrylamide (w/v), 0.3−0.5% *N*,*N*′-methylenebisacrylamide (w/v), 0.03% *N*,*N*,*N*′,*N*′-tetramethylethylenediamine (v/v), and 0.05% ammonium persulfate (w/v). These are very similar to the concentrations of components previously reported.[8,34,35] Prior to the addition of the gel initiator, concentrated LH2 membranes having an optical density (OD) of approximately 60 at 800 nm were added to the gel solution to obtain a final OD of 1.0 at 800 nm. The gels were allowed to form on ice in 5 cm long, 0.9 cm inside diameter, cylindrical glass tubes that had been sealed at one end. After the gels were set in approximately 3 h, they were extracted from the tubes by sliding a narrow gauge needle between the gel and the glass tube and injecting water behind the gel. The gels were then sliced with a razor blade into 4 cm long sections and allowed to dry in air for a few minutes before placing them in the cuvettes.

Sample Orientation, Absorption, and LD. Orientation of the LH2 membranes was achieved by squeezing the gels in 1 cm polymethacrylate (nonbirefringent) cuvettes (Sigma model C-0793) to approximately 60% of the original volume, as previously described.[35] A square steel plunger with a flat rubber base was used to compress the gel in the cuvette and to maintain a constant pressure on the gel for the duration of the absorption and LD measurements.

Absorption and LD measurements used a Cary 50 UV/vis spectrophotometer on samples at room temperature. A prism polarizer placed in the path of the incident light was mounted on a graduated rotating base that could be dialed to generate plane-polarized light at various angles relative to the squeeze axis of the sample. Polarized absorption spectra were taken at angles of 0°, 30°, 60° and 90°. The polarized absorption spectra were corrected for scattering by using a simplex algorithm that removed scattering so that the correction satisfied two criteria. First, the scattering correction had to satisfy the simple formula $a + b\lambda^4$, where a and b are independent variables. We made the further assumption that the scattering correction was identical (isotropic) at all polarization angles. The latter assumption allowed a simplex fit of the function with the requirement that the region from 650 to 750 nm have a net slope of zero. This region is largely devoid of absorption bands and in the absence of scattering, should be flat except for the small band centered at $\sim$700 nm. When the same correction for all polarization angles is assumed, we prevent the scattering correction from having an influence on the calculation of the transition dipole moment.

Results

Experimentally Observed LD. Figure 4 shows the dependence of the intensity of absorption on the angle of the polarizer for the B800 Q_y, B850 Q_y, and rhodopin glucoside transitions. The spectra were taken on LH2 membranes from *R. acidophila* in squeezed gels prepared as described in the Materials and Methods section. Figure 4 shows that the absorption intensity increases when the polarizer is rotated from 0 to 90° in both the B800 Q_y and B850 Q_y regions, and decreases in the rhodopin glucoside absorption region of the spectrum ($\sim$450−550 nm). Because of the limitations in the signal-to-noise ratio of the instrument, the spectra were subjected to a 10-point digital smoothing algorithm prior to computing the LD and LD-to-isotropic absorption (LD/A) spectra shown in Figure 5, which were otherwise obtained directly from the data presented in Figure 4. The smoothing did not affect the relative intensities of the spectra in any statistically significant way. The isotropic absorption spectrum used to compute the LD/A profile was

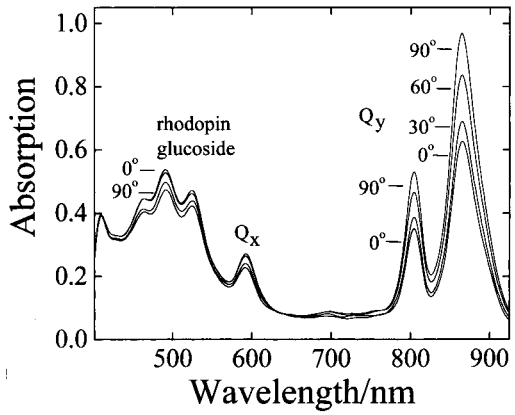

Figure 4. Polarized absorption spectra of the LH2 complex from *R. acidophila* strain 10050 squeezed in a polyacrylamide gel. The spectra were taken at room temperature with the polarizer having angles of 0, 30, 60, and 90° with respect to the squeeze direction. The spectra were subjected to a 10-point smoothing algorithm to reduce the small amount of random noise present in the traces.

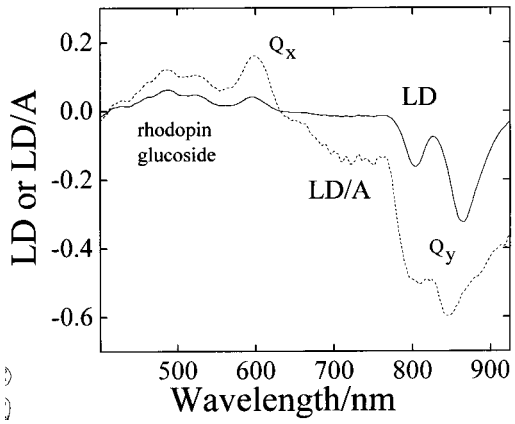

Figure 5. LD (solid line) and LD/A (dashed line) spectra of the LH2 complex from *R. acidophila* strain 10050 squeezed in a polyacrylamide gel. The LD spectrum was computed from the difference between the 0 and the 90° spectra given in Figure 3 after the data were subjected to a 10-point smoothing algorithm. The LD/A spectrum was computed by dividing the LD spectrum by an isotropic absorption spectrum obtained from an unoriented membrane preparation having the same concentration as that used in the squeezed gels.

obtained from an unoriented membrane preparation having the same concentration as that used in the squeezed gels. The LD/A values for the B800 Q_y, and B850 Q_y transitions are strongly negative, whereas the value for the rhodopin glucoside transition is slightly positive. It should be mentioned that the absorption band at 850 nm contains a contribution from the RC-LH1 core complex whose peak absorption is near 875 nm. Because the spectra of the membranes in solution do not show a substantial contribution from the RC-LH1 protein, it can be concluded that the LH2 protein is present in a vast excess. Thus, the ensuing discussion assumes that the contribution from the RC-LH1 protein is negligible at 850 nm as compared to the B850 BChl Q_y absorption associated with the LH2 protein. Also, the large positive feature near 600 nm corresponds to a composite peak associated with the Q_x transitions from both B800 and B850 absorbing BChls. The data presented here are not sufficiently resolved to distinguish the spectra associated with the different pigments in this region. Hence, the Q_x transitions will not be discussed further.

Semiempirical MO Computations. To calculate the transition moment direction of the protein-bound rhodopin glucoside chromophore, the semiempirical MO procedures that have been

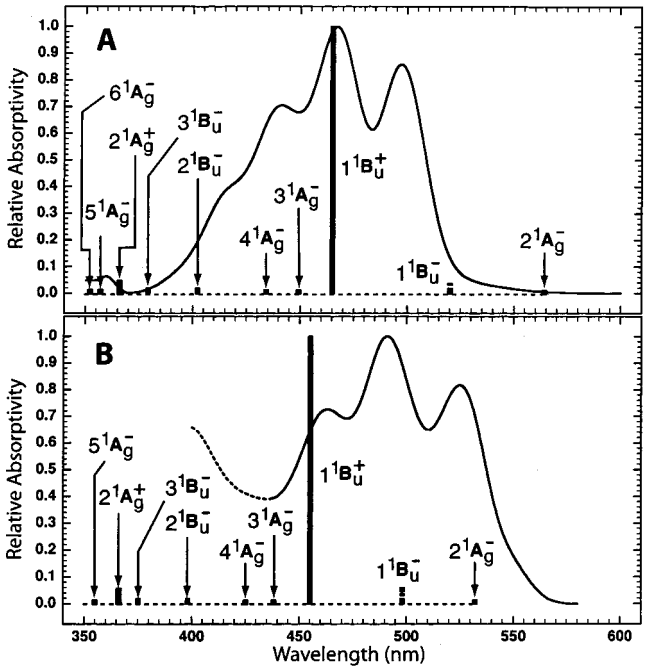

Figure 6. Comparison of the MNDO−PSDCI calculated transition energies and oscillator strengths with the observed absorption spectra of rhodopin glucoside in pentane (A) and in the native LH2 complex from *R. acidophila* strain 10050 (B). The height of the vertical bars is proportional to oscillator strength, and the symmetry labels are approximate.

shown to provide accurate transition moments of long chain linear and substituted polyenes were adopted.[30,9] MNDO−PSDCI MO theory is used with full single CI and partial double CI over the π-system of the polyene chromophore.[29] We have developed spectroscopic parametrizations that work with the MNDO, AM1, or PM3 Hamiltonians,[9,29−31,37−40] and the present calculations use the PM3 Hamiltonian. A key observation of our previous studies is that if the MNDO−PSDCI method reproduces the transition energy within the Franck−Condon envelope, it yields a transition moment vector within experimental error provided high-level double CI is included to properly correlate the wave function.[9,30] We included all possible single excitations and the 5000 lowest energy doubly excited states, more than twice that necessary to yield a convergence of the $^1B_u^+$-like state properties to within 0.2% of their final values with full single and double CI.

We compare the calculated transition energy of the $^1B_u^+$-like state ($\Delta E = 2.66$ eV, $f = 2.8$, 6% doubly excited) with the absorption spectrum of rhodopin glucoside in pentane in Figure 6. The agreement is fortuitously excellent. Normally, the MNDO−PSDCI transition energies are 0.2 eV above those measured in hydrocarbon solvent.[9,29−31,37−40] The calculations predict two excited states below this $^1B_u^+$-like state, a weakly allowed $^1B_u^-$-like state ($\Delta E = 2.38$ eV, $f = 0.05$, 78% doubly excited) and a forbidden $^1A_g^-$-like state ($\Delta E = 2.19$ eV, $f = 0.001$, 78% doubly excited). The reliability of the $^1B_u^+$-like state assignment is less certain, but it should be noted that MNDO−PSDCI theory reproduces ab initio effective Hamiltonian level ordering for the shorter polyenes with accuracies of better than 0.3 eV.[29] This state is not an artifact of semiempirical MO theory. Also, there is strong evidence to support a lowest-lying $^1A_g^-$-like state in this long chain polyene (for a review, see ref 41).

The challenge for the present study is that the chromophore is confined to a protein binding site that forces the chromophore to adopt a nonlinear "corkscrewlike" geometry.[32] We carried

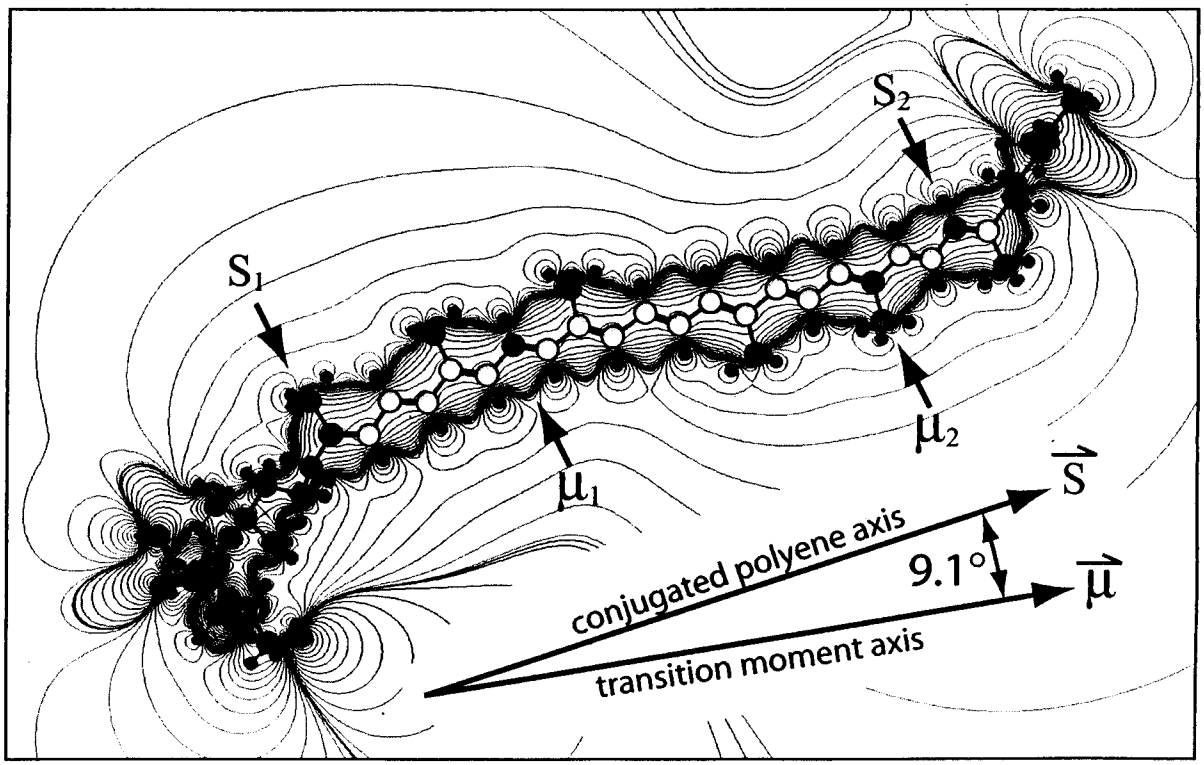

Figure 7. Structure of the optimized rhodopin glucoside molecule depicting the directions of the long structural axis, $\vec{S}$, and the transition moment vector, $\vec{\mu}$. The structure axis lies along the two points designated S_1 and S_2, which correspond to the first and last carbon in the π-electron conjugation. The transition moment vector lies along the points labeled μ_1 and μ_2. The wavy lines represent the contours of electron density.

out an initial MNDO−PSDCI calculation on the X-ray coordinates of the chromophore, but as was anticipated, the relatively low-resolution structure yielded a highly strained ground state geometry, and the calculated transition energies were unrealistic. At the same time, a fully minimized structure, where the minimization is carried out in a vacuum, yields a transition moment of little relevance to the protein-induced chromophore conformation. We solved the problem by carrying out a semiempirical (PM3 Hamiltonian) minimization within the protein binding site while holding the coordinates of all residues fixed and allowing the chromophore to relax fully. The coordinates of the relaxed rhodopin glucoside structure are presented in Table S1. At low resolution, the minimized and original X-ray geometries overlap perfectly, but on close inspection, significant differences in bond lengths and bond angles are observed. The protein-bound relaxed chromophore has electronic properties calculated to be quite similar to the isolated chromophore, and the two spectra are compared in Figure 6. The small blue shift in the calculated transition energies is traced to preferential torsional distortion about the single bonds (rather than the double bonds) of the polyene chain. Because electronic excitation induces a small degree of bond order reversal, single bond distortions yield blue shifts due to destabilization of the excited state. Conversely, double bond distortions induce a red shift. Single bond distortions induce larger blue shifts in those transitions with higher degrees of doubly excited character because the respective excited states experience larger bond order reversal. There are still two states calculated to lie below the strongly allowed $^1B_u^+$-like state in the protein-bound rhodopin glucoside chromophore. The weakly allowed $^1B_u^-$-like state ($\Delta E = 2.49$ eV, $f = 0.11$, 76% doubly excited) and the forbidden $^1A_g^-$-like state ($\Delta E = 2.33$ eV, $f = 0.0004$, 78% doubly excited) are both blue-shifted by roughly 0.12 eV relative to the isolated chromophore. In comparison, the $^1B_u^+$-like state ($\Delta E = 2.72$ eV, $f = 2.7$, 8% doubly excited) is blue-shifted by only 0.06 eV.

While the protein-bound chromophore is calculated to have slightly higher transition energies, the spectrum of the protein-bound chromophore (Figure 1B) is red-shifted. We believe that this red shift is due primarily to a dispersive shift associated with the protein binding site coupled with a smaller electrostatic shift. Regardless of origin, the shift is not large enough to have much impact on the calculated transition moment, which to first order, is not affected by dispersive or electrostatic shifts of the parent excitation. A small correction in the transition moment direction was introduced based on the reaction field associated with the protein cavity. The origin of the reaction field correction has been described previously.[9,42] The present calculation yielded a transition moment direction for the carotenoid in the plane of the π-electron conjugated system at an angle of 9.1° relative to a vector drawn from the first carbon in the conjugated chain (point S_1 in Figure 7) to the last (point S_2 in Figure 7).

Hudson and co-workers have examined the angle of the transition dipole moment relative to the polyene long axis in a series of polyenes with up to 11 double bonds.[9] Of particular note is the angle observed (15°) and calculated (14.6°) for lycopene, a carotenoid with the same number of conjugated double bonds as rhodopin glucoside. It is instructive to compare the present theoretical prediction of a 9.1° transition moment angle with the 14.6° angle calculated for lycopene. The difference is due primarily to the geometry imposed on the chromophore by the protein binding site. Indeed, when the geometry of rhodopin glucoside is minimized in a vacuum or in a solvent (using COSMO), a transition moment is calculated that is 14.7° off axis, nearly identical to the value calculated for lycopene. This observation confirms the importance of the protein matrix in constraining the off-axis direction of the transition moment.

LD Expected from the Crystal Structure. The observed LD will result from an average of the contributions from the nine different pigment−protein units comprising the ring of the circular LH2 complex. The individual contributions are determined using the site permutation matrix

$$\hat{R} = \begin{vmatrix} \cos\theta & \sin\theta & 0 \\ -\sin\theta & \cos\theta & 0 \\ 0 & 0 & 1 \end{vmatrix} \quad (1)$$

that rotates one of the components by 40° (i.e., 360°/9) into the next. Application of this rotation operation requires transformation of the coordinates of the pigments from the crystal structure unit cell coordinate system into the laboratory coordinate system. To accomplish this, we define the laboratory *Z*-axis as the vertical dimension of the cuvette, which is also coincident with the squeeze direction, the 0° orientation of the polarizing crystal, and the membrane normal, denoted $\vec{N}$. It is known from the crystal structure that the molecular axis, corresponding to a line connecting rings II and IV nitrogens (Figure 2) of the 850 nm absorbing BChls, lies on average, parallel to $\vec{N}$.[33] Thus, the matrix, $\hat{T}$, for the transformation from the crystalline unit cell coordinates into the laboratory frame, can be constructed by finding the Euler matrix elements that satisfies

$$\hat{T} \cdot \vec{B} = \vec{V} \quad (2)$$

where

$$\hat{T} = \begin{vmatrix} \cos\theta\cos\chi - \sin\phi\cos\theta\sin\chi & -\cos\theta\sin\chi - \sin\phi\cos\theta\cos\chi & \sin\phi\sin\theta \\ \sin\phi\cos\chi + \cos\phi\cos\theta\sin\chi & -\sin\phi\sin\chi + \cos\phi\cos\theta\cos\chi & -\cos\phi\sin\theta \\ \sin\theta\sin\chi & \sin\theta\cos\chi & \cos\theta \end{vmatrix}$$

and $\vec{B}$ is the average direction of the ring II to ring IV, nitrogen−nitrogen molecular axis of the 850 nm absorbing BChls in the crystalline unit cell axis system, and $\vec{V}$ has the coordinates (0,0,1). The vector $\vec{B}$ was derived from averaging the molecular axis directions computed from the vectors that connect the nitrogen atoms in rings II and IV (Figure 2) of all 18 B850 BChl molecules in the crystal structure. The vector computed in this manner was $\vec{B} = (-0.339, 0.915, 0.217)$. The angles $\phi = -80.2°$, $\theta = 91.7°$, and $\chi = -24.1°$ were found by iterative methods to satisfy the relation given by eq 2.

The intensity of polarized absorption is proportional to the sum of the squares of the dot products of the transition moment vectors, transformed into the laboratory axis system, and to the electric vector of the incident radiation polarized either parallel or perpendicular to the squeeze direction.

$$A_{||} \propto \sum_{i=1}^{9} (\hat{R} \cdot \hat{T} \cdot \vec{\mu}_i \cdot \vec{E}_{||})^2 \quad (3)$$

$$A_{\perp} \propto \sum_{i=1}^{9} (\hat{R} \cdot \hat{T} \cdot \vec{\mu}_i \cdot \vec{E}_{\perp})^2 \quad (4)$$

Here, $\vec{\mu}_i$ represents the transition moment of an absorbing pigment occupying site $i = 1$ through 9 around the ring. $\vec{E}_{||}$ is represented by the vector (0,0,1), and $\vec{E}_{\perp}$ is either (1,0,0) or (0,1,0). By definition, LD is expressed as the difference between light absorbed with the polarizer parallel and perpendicular to the squeeze direction.

$$\mathrm{LD} = A_{||} - A_{\perp} \quad (5)$$

If the LD is divided by *A*, the absorption of an isotropic, unoriented sample, the following expression can be written:

$$\frac{\mathrm{LD}}{A} = \left\langle \frac{3}{2}(3\cos^2\alpha - 1) \right\rangle p \quad (6)$$

where α is the angle between the transition dipole moment of an absorbing molecule and the axis of orientation, i.e., the normal to the membrane, and *p* is a parameter that describes the average extent of ordering.[43]

B800 Q_y Transition Moment. As a first approximation, the Q_y transition moment of the 800 nm absorbing BChls was assumed to be described by a vector connecting the nitrogen atoms in rings I and III (Figure 2) of the B800 BChl macrocycles. The LD/A value for the B800 Q_y transition at 800 nm was then computed from the crystal structure by transforming this vector from the unit cell coordinates into the laboratory axis system using eq 2. The resulting normalized vector, $\vec{B}800 = (-0.998,-0.031,-0.059)$, was then used in eqs 3−5, and assuming an isotropic absorption $A = (A_{||} + 2A_{\perp})/3$, the LD/A was computed to be −1.48. This corresponds to an angle, α, of 89° between the B800 Q_y transition moment and the normal to the membrane. It has been suggested that the Q_y transition moments of some chlorophyll derivatives may be slightly off axis from the molecular axis system defined by the positions of the nitrogens, and that the Q_x and Q_y transition moments may not be strictly orthogonal.[44,45] Most investigators believe the transition moments and molecular axes to be coincident within at least a few degrees.[46−50] The possibility that the transition moment does not coincide precisely with the molecular axis defined by the positions of the nitrogens was explored by rotating the direction of the transition moment in the plane of the 800 nm absorbing BChl macrocycle and recalculating the LD/A. Rotating the transition moment by up to 15°, which is more than the maximum amount suggested by the experimental and theoretical studies reported in the literature, changed the value of the predicted LD/A by less than 0.1, and had negligible effect on the computed angle that the transition moment makes with respect to the membrane normal. This is not surprising because the plane of the 800 nm absorbing BChl macrocycle lies largely in the plane of the membrane.[33]

B850 Q_y Transition Moment. The Q_y transition of the 850 nm absorbing BChls can also be described, to a first approximation, by a vector connecting the nitrogen atoms in rings I and III (Figure 2) of the B850 BChl macrocycles.[50] The LD/A value for this transition was calculated in the same manner as described for the B800 Q_y transition moment. The normalized, transformed vector, $\vec{B}850$, was found to have the coordinates $(-0.965,-0.261,-0.030)$, and the value of the LD/A was computed to be −1.50, which corresponds to an angle of 90° for this transition moment with respect to the membrane normal. Once again, the possibility that the transition moment does not coincide precisely with the molecular axis defined by the positions of the nitrogens was explored by rotating its direction in the plane of the 850 nm absorbing BChls and recalculating the LD/A. As in the case of the 800 nm absorbing BChl, a rotation of up to 15° only changed the value of the predicted LD/A by less than 0.1. This had negligible effect on the predicted angle of the transition moment with respect to the membrane normal.

Rhodopin Glucoside Transition Moment. The rhodopin glucoside molecule follows a twisted-sigmoidal path through the protein (Figure 3). We define the long axis of the carotenoid structure as a vector, $\vec{S}$, directed through the molecule from the first carbon in conjugation (point S_1 on Figure 7) to the last (point S_2 on Figure 7). The semiempirical MO calculations

TABLE 1: LD/A Values and Angles, α, between the Transition Moment and the Squeeze Direction Obtained Experimentally and Computed from the Coordinates of the Crystal Structure of the LH2 Complex from *R. acidophila* 10050[a]

	experimental		cryst structure		ratio of experimental and cryst structure
	LD/A	α (deg)	LD/A	α (deg)	LD/A
rhodopin glucoside, $\vec{\mu}$	0.10 ± 0.05	53.4 ± 0.7	0.67	46	0.15 ± 0.08
B800 Q_y	−0.54 ± 0.05	62.5 ± 0.8	−1.48	89	0.36 ± 0.04
B850 Q_y	−0.57 ± 0.05	62.9 ± 0.8	−1.50	90	0.38 ± 0.03
rhodopin glucoside, $\vec{S}$			0.38	50	

[a] The errors in the experimental numbers are based on the signal-to-noise ratio inherent in the spectra. The values of α are computed using eq 6 in the text and assume perfect ordering; i.e., $p = 1$. The values of LD/A are calculated from the crystal structure for the two cases: (1) Rhodopin glucoside, $\vec{\mu}$, for the transition moment rotated 9.1° from the structure axis and (2) Rhodopin glucoside, $\vec{S}$, assuming the transition moment is aligned along the structure axis of the carotenoid.

described above predict the transition dipole moment of the strongly allowed $1^1A_g^- \rightarrow 1^1B_u^+$ transition to be rotated 9.1° away from the $\vec{S}$ structural axis and coincident with a line drawn from points μ_1 to μ_2 along the conjugated π-electron chain (Figure 7). We denote the transition moment vector $\vec{\mu}$.

The crystal coordinates for the rhodopin glucoside transition moment, $\vec{\mu}$, were transformed from the unit cell axis system into the laboratory axis system using eq 2. The normalized, transformed, transition moment vector was found to have the coordinates $\vec{\mu} = (0.596, 0.502, -0.695)$. Using the procedure described above for the B800 and B850 absorbing BChls that involved summing the contributions to the polarized absorption spectra from the nine units of the protein ring, the value of the LD/A for rhodopin glucoside was computed to be +0.67. This corresponds to an angle, α, of 46° between the transition moment of the carotenoid and the membrane normal. This is completely consistent with previous findings on the LH2 complex from *Rhodobacter sphaeroides* 2.4.1.[8,4]

The model allows an exploration of how the LD/A, predicted from the crystal structure, depends on the angle the transition moment has with respect to the carotenoid structure axis. If it is assumed that the carotenoid transition moment is collinear with the structure vector, $\vec{S}$, (Figure 7) then after this vector is transformed and the contributions are summed to the polarized absorption from each of the nine sites in the protein, the LD/A for the rhodopin glucoside is computed to be +0.38. This corresponds to an angle of 50° for the rhodopin glucoside transition moment with respect to the membrane normal. The experimental and computed LD/A values and angles for the rhodopin glucoside, B800 Q_y, and B850 Q_y transitions are summarized in Table 1.

Discussion

Comparison of Computed and Experimental LD. The data presented in Table 1 show that the LD/A values computed from the LH2 crystal structure are numerically larger than those observed experimentally from the complex squeezed in a polyacrylamide gel. The simple explanation for this is that the structure of the LH2 complex derived from X-ray diffraction methods necessarily requires a highly ordered crystalline sample. Significant crystalline disorder would preclude the use of X-ray methods to solve the structure to atomic resolution in the first place. Hence, the polarized absorption effects predicted from coordinates derived from X-ray diffraction are expected to be at or near the maximum observable.

Spectroscopic studies on crystals from the *R. acidophila* 10050 LH2 complex and other preparations from photosynthetic organisms have been reported,[51−57] but the ability to extract useful information regarding the orientation of the transition moment vectors of the pigments with respect to the molecular structure axes and otherwise interpret the data has been hindered by several factors including, the need to use very thin crystals, the problem of verifying the crystalline form used in the spectroscopic experiments, macroscopically aligning the crystals, and the fact that more than one pigment−protein complex typically exists per unit cell. This last factor introduces an almost insurmountable complication to solving the problem of correlating the transition moment directions with molecular structure. In principle, if the crystalline symmetry is known, the corresponding site permutation matrixes can be applied to generate the associated spectral response. In practice, however, the more protein complexes per unit cell, the larger the number of mathematically valid solutions to the problem. A few investigators have combined LD data from single crystals and membranes with data from magnetophotoselection[58−60] and single crystal electron paramagnetic resonance experiments[61] in an attempt to narrow the region of solution.

The experimental LD data presented here are taken on LH2 complexes that are bound in large, planar sheets of membranes isolated from the bacterium and squeezed in gels. Squeezing the membranes in polyacrylamide gels will not induce perfect ordering due to irregularities in the structures of the gels and the membranes and in the manner in which the membranes stack when compressed. However, the pronounced LD and LD/A shown in Figure 5 suggest a reasonably high degree of ordering. The magnitude of the effects observed experimentally are smaller than those predicted from the crystal structure, but the trends in the data are consistent with each other: The signs of the experimental and computed LD are both negative for the B800 Q_y and B850 Q_y and positive for the rhodopin glucoside transitions, and in both cases, the LD/A values for the B800 Q_y and B850 Q_y transitions are significantly more negative than the rhodopin glucoside LD/A values are positive. Moreover, for all three transitions the ratio of the experimental LD/A value to the LD/A value computed from the crystal structure lies within the narrow range of 0.3 ± 0.15. This suggests that the difference between the experimental results and those predicted from the crystal structure may be attributed to partial randomization in the stacking of the membranes as the sole source of disorder, and that a narrow range of values for the order parameter, p, in eq 6 may account for this difference across the entire LD/A spectrum.

Effect of the Transition Moment Direction on the LD/A. In the literature dealing with carotenoids in proteins and membranes, it has been tacitly assumed that the transition moment lies along the long structural axis of the molecule. As mentioned above, there is no symmetry requirement that this be the case. The off-axis angle can take on any value and still adhere to the symmetry operations that comprise the point group.[9] Our semiempirical MO computational methods predict the off-axis angle for rhodopin glucoside to be 9.1°. As shown in the Results section, this orientation of the transition moment

yields a computed value of +0.67 for the LD/A. If one assumes that the transition moment is aligned with the long axis of the molecule, the LD/A value for the rhodopin glucoside is computed to be +0.38. Thus, a rotation of 9.1° in the direction of the transition moment is shown here to lead to an almost factor of 2 difference in the predicted LD/A. This is a significant effect that has not previously taken into account when LD has been used to elucidate the structures of carotenoids in biological proteins and membranes. Although the LD/A values are significantly different for the two cases, the average angles, α, derived from the expression given in eq 6, assuming perfect ordering (i.e., $p = 1$), are not. In the case where the transition moment is off axis, the transition moment makes an angle of 46° with the membrane normal. If the transition moment is along the long axis of the carotenoid, the angle is 50°. This insensitivity of the angle to the value of LD/A is directly traceable to the algebraic form of eq 6.[2] The functional nature of the $(3 \cos^2 \alpha - 1)$ term is such that in the region around 54.7°, the magic angle where the function crosses zero and its slope is steepest, there can be a large change in LD/A that corresponds to only a small change in the angle, α. At angles near 0 or 90°, small changes in LD/A may have a significant effect on the value of α. It is only by fortuitous circumstances in the LH2 complex, where the carotenoid is tilted at an angle of approximately 50°, that the large differences in LD/A values do not manifest themselves in significantly different predictions for the angle of the transition moment with respect to the membrane normal. If the carotenoid was to lie more in the plane of the membrane, as it does in photosynthetic reaction centers,[62,63] or if the alignment axis is different, the structures and geometries of carotenoids based on experimental LD/A values may be systematically in error.

Semiempirical MO computations have shown that the transition moment of the rhodopin glucoside is 9.1° off axis from the long, structural axis of the molecule. It is expected that all carotenoids have a similar degree of rotation of their strongly allowed electronic transition moments with respect to the long axis of π-electron conjugation.[9] This rotation is a function of the single/double bond alternation present in carotenoids. It does not originate from binding the carotenoid to the protein, but its magnitude may be modulated by interactions with the environment. The fact that the transition moment associated with the strongly allowed $1^1A_g \rightarrow 1^1B_u^+$ transition in carotenoids is generally not collinear with the long structure axis should be considered when LD or any polarized light spectroscopic method is used to elucidate the structures and geometries of these molecules in biological systems.

Acknowledgment. This work has been supported in the laboratory of H.A.F. by grants from the National Science Foundation (MCB-9816759), the National Institute of Health (GM-30353), and the University of Connecticut Research Foundation. R.R.B. acknowledges partial support for this work through a grant from the National Institute of Health (GM-34548). Support for R.J.C. has been provided by the BBSRC. H.A.F. and R.J.C. also acknowledge a NATO grant for International Collaboration. Funding for D.M. was provided by an NSF Research Experience for Undergraduates (REU) program (CHE-9732366) at the University of Connecticut.

Supporting Information Available: Table S1 showing the coordinates of the protein-bound, relaxed rhodopin glucoside structure. This material is available free of charge via the Internet at http://pubs.acs.org.

References and Notes

(1) Hofrichter, J.; Eaton, W. A. *Annu. Rev. Biophys. Bioeng.* **1976**, *5*, 511−560.
(2) Breton, J.; Vérméglio, A. Orientation of Photosynthetic Pigments in Vivo. In *Photosynthesis*: *Energy Conversion by Plants and Bacteria*; Govindjee, Ed.; Academic Press: New York, 1982; Vol. 1, pp 153−194.
(3) Paillotin, G.; Vérméglio, A.; Breton, J. *Biochim. Biophys. Acta* **1979**, *545*, 249−264.
(4) Kramer, H. J. M.; van Grondelle, R.; Hunter, C. N.; Westerhuis, W. H. J.; Amesz, J. *Biochim. Biophys. Acta* **1984**, *765*, 156−165.
(5) Breton, J.; Michel-Villaz, M.; Paillotin, G. *Biochim. Biophys. Acta* **1973**, *314*, 42−56.
(6) Vérméglio, A.; Breton, J.; Paillotin, G.; Cogdell, R. *Biochim. Biophys. Acta* **1978**, *501*, 514−30.
(7) Breton, J. *Biochim. Biophys. Acta* **1985**, *810*, 235−245.
(8) Breton, J.; Nabedryk, E. Pigment and Protein Organization in Reaction Center and Antenna Complexes. In *The Light Reactions*; Barber, J., Ed.; Elsevier Science Publishers B. V.: Amsterdam, 1987; pp 159−195.
(9) Birge, R. R.; Zgierski, M. Z.; Serrano-Andres, L.; Hudson, B. S. *J. Phys. Chem. A* **1999**, *103*, 2251−2255.
(10) Hudson, B. S.; Kohler, B. E.; Schulten, K. Linear Polyene Electronic Structure and Potential Surfaces. In *Excited States*; Lim, E. D., Ed.; Academic Press: New York, 1982; Vol. 6, pp 1−95.
(11) Hudson, B. S.; Kohler, B. E. *Synth. Met.* **1984**, *9*, 241−253.
(12) Kohler, B. E. Electronic Properties of Linear Polyenes. In *Conjugated Polymers*: *The Novel Science and Technology of Conducting and Nonlinear Optically Active Materials*; Bredas, J. L., Silbey, R., Eds.; Kluwer Press: Dordrecht, The Netherlands, 1991.
(13) Kohler, B. E. Carotenoid Electronic Structure. In *Carotenoids*; Pfander, H., Liaaen-Jensen, S., Britton, G., Eds.; Birkhäuser Verlag AG: Basel, 1993; Vol. 1B.
(14) Granville, M. F.; Holtom, G. R.; Kohler, B. E.; Christensen, R. L.; D'Amico, K. L. *J. Chem. Phys.* **1979**, *70*, 593−597.
(15) D'Amico, K. L.; Manos, C.; Christensen, R. L. *J. Am. Chem. Soc.* **1980**, *102*, 4671−4675.
(16) Snyder, R.; Arvidson, E.; Foote, C.; Harrigan, L.; Christensen, R. L. *J. Am. Chem. Soc.* **1985**, *107*, 4117−4122.
(17) Simpson, J. H.; McLaughlin, L.; Smith, D. S.; Christensen, R. L. *J. Chem. Phys.* **1987**, *87*.
(18) Kohler, B.; Westerfield, C. *J. Chem. Phys.* **1988**, *89*, 5422−5428.
(19) Birge, R. R. *Acc. Chem. Res*. **1986**, *19*, 138−146.
(20) Pariser, R. *J. Chem. Phys.* **1955**, *24*, 250−268.
(21) Callis, P. R.; Scott, T. W.; Albrecht, A. C. *J. Chem. Phys.* **1983**, *78*, 16−22.
(22) Koyama, Y.; Fujii, R. Cis−Trans Carotenoids in Photosynthesis: Configurations, Excited-State Properties and Physiological Functions. In *The Photochemistry of Carotenoids*; Frank, H. A., Young, A. J., Britton, G., Cogdell, R. J., Eds.; Kluwer Academic Publishers: Dordrecht, 1999; Vol. 8, pp 161−188.
(23) *The Photochemistry of Carotenoids*; Frank, H. A., Young, A. J., Britton, G., Cogdell, R. J., Eds.; Kluwer Academic Publishers: Dordrecht, 1999; Vol. 8.
(24) Hudson, B. S.; Kohler, B. E. *Chem. Phys. Lett.* **1972**, *14*, 299−304.
(25) Schulten, K.; Karplus, M. *Chem. Phys. Lett.* **1972**, *14*, 305−309.
(26) Ohmine, I.; Karplus, M.; Schulten, K. *J. Chem. Phys.* **1978**, *68*, 2298−2318.
(27) Schulten, K.; Ohmine, I.; Karplus, M. *J. Chem. Phys.* **1976**, *64*, 4422−4441.
(28) Hudson, B.; Kohler, B. *Annu. Rev. Phys. Chem.* **1974**, *25*, 437−460.
(29) Martin, C. H.; Birge, R. R. *J. Phys. Chem. A* **1998**, *102*, 852−860.
(30) Hudson, B. S.; Birge, R. R. *J. Phys. Chem. A* **1999**, *103*, 2274−2281.
(31) Kusnetzow, A.; Singh, D. L.; Martin, C. H.; Barani, I.; Birge, R. R. *Biophys. J.* **1999**, *76*, 2370−2389.
(32) McDermott, G.; Prince, S. M.; Freer, A. A.; Hawthornthwaite-Lawless, A. M.; Papiz, M. Z.; Cogdell, R. J.; Isaacs, N. W. *Nature* (*London*) **1995**, *374*, 517−521.
(33) Freer, A.; Prince, S.; Sauer, K.; Papiz, M.; Hawthornthwaite-Lawless, A.; McDermott, G.; Cogdell, R.; Isaacs, N. W. *Structure* (*London*) **1996**, *4*, 449−462.
(34) Haworth, P.; Tapie, P.; Arntzen, C. J.; Breton, J. *Biochim. Biophys. Acta* **1982**, *682*, 152−159.
(35) Abdurakhmanov, I. A.; Ganago, A. O.; Erokhin, Y. E.; Solov'ev, A. A.; Chugunov, V. A. *Biochim. Biophys. Acta* **1979**, *546*, 183−186.
(36) Cogdell, R. J.; Durant, I.; Valentine, J.; Lindsay, J. G.; Schmidt, K. *Biochim. Biophys. Acta* **1983**, *722*, 427−35.

(37) Stuart, J. A.; Vought, B. W.; Zhang, C. F.; Birge, R. R. *Biospectroscopy* **1995**, *1*, 9−28.
(38) Tallent, J. R.; Birge, J. R.; Zhang, C. F.; Wenderholm, E.; Birge, R. R. *Photochem. Photobiol.* **1992**, *56*, 935−952.
(39) Tallent, J. R.; Hyde, E. Q.; Findsen, L. A.; Fox, G. C.; Birge, R. R. *J. Am. Chem. Soc.* **1992**, *114*, 1581−1592.
(40) Barlow, R.; Birge, R.; Kaplan, E.; Tallent, J. *Nature* **1993**, *366*, 64−66.
(41) Frank, H. A. *Arch. Biochem. Biophys.*, in press.
(42) Shang, Q.-Y.; Dou, X.; Hudson, B. S. *Nature* **1991**, *352*, 703.
(43) Kleima, F. J.; Wendling, M.; Hofmann, E.; Peterman, E. J. G.; van Grondelle, R.; van Amerongen, H. *Biochemistry* **2000**, *39*, 5184−5195.
(44) Fragata, M.; Nordén, B.; Kurucsev, T. *Photochem. Photobiol.* **1988**, *47*, 133−143.
(45) Petke, J. D.; Maggiora, G. M.; Shipman, L.; Christoffersen, R. E. *Photochem. Photobiol.* **1979**, *30*, 203−223.
(46) Weiss, C. *J. Mol. Spectrosc.* **1972**, *44*, 37−80.
(47) Chang, J. C. *J. Chem. Phys.* **1977**, *67*, 3901−3909.
(48) Kuki, A.; Boxer, S. G. *Biochemistry* **1983**, *22*, 2923−2933.
(49) Moog, R. S.; Kuki, A.; Fayer, M. D.; Boxer, S. G. *Biochemistry* **1984**, *23*, 1564−1571.
(50) Scherz, A.; Parson, W. W. *Photosynth. Res.* **1986**, *9*, 21−32.
(51) Frank, H. A.; Violette, C. A.; Taremi, S. S.; Budil, D. E. *Photosynth. Res.* **1989**, *21*, 107−116.
(52) Frank, H. A.; Aldema, M. L.; Parot, P. H.; Cogdell, R. J. *Photosynth. Res.* **1990**, *26*, 93−99.
(53) Frank, H. A.; Aldema, M. L.; Violette, C. A.; Parot, P. H. *Photochem. Photobiol.* **1991**, *54*, 151−155.
(54) Frank, H. A.; Aldema, M. L. *Correlation between the Polarized Light Absorption and the X-ray Structure of Single Crystals of the Reaction Center from Rhodobacter sphaeroides R-26*; Photosynthetic Bacterial Reaction Center II: Cadarache, France, 1992.
(55) Taremi, S. S.; Violette, C. A.; Frank, H. A. *Biochim. Biophys. Acta* **1989**, *973*, 86−92.
(56) Aldema, M. A. *Spectroscopic Studies of Crystalline Photosynthetic Complexes*; University of Connecticut: Storrs, CT, 1992.
(57) Steck, K.; Wacker, T.; Drews, G.; Gad'on, N.; Cogdell, R.; Welte, W.; Mantele, W. *Curr. Res. Photosynth., Proc. Int. Conf. Photosynth., 8th* **1990**, *2*, 121−124.
(58) Frank, H. A.; Bolt, J.; Friesner, R.; Sauer, K. *Biochim. Biophys. Acta* **1979**, *547*, 502−511.
(59) Trosper, T. L.; Frank, H. A.; Norris, J. R.; Thurnauer, M. C. *Biochim. Biophys. Acta* **1982**, *679*, 44−50.
(60) McGann, W. J.; Frank, H. A. *Biochim. Biophys. Acta* **1985**, *807*, 101−109.
(61) Budil, D. E.; Taremi, S. S.; Gast, P.; Norris, J. R.; Frank, H. A. *Isr. J. Chem.* **1988**, *28*, 59−66.
(62) Yeates, T. O.; Komiya, H.; Chirino, A.; Rees, D. C.; Allen, J. P.; Feher, G. *Proc. Natl. Acad. Sci. U.S.A.* **1988**, *85*, 7993−7997.
(63) Arnoux, B.; Ducruix, A.; Reiss-Husson, F.; Lutz, M.; Norris, J.; Schiffer, M.; Chang, C.-H. *FEBS Lett.* **1989**, *258*, 47−50.